An Efficient Equalization Method to Minimize Delay Spread in OFDM/DMT Systems

Romed Schur and Joachim Speidel
Institut für Nachrichtenübertragung
Universität Stuttgart, Pfaffenwaldring 47, 70569 Stuttgart, Germany
Email: schur@inue.uni-stuttgart.de

***Abstract*– A time domain equalization technique to be used in an Orthogonal Frequency Division Multiplex (OFDM) or Discrete Multi Tone (DMT) system is proposed, which directly minimizes the delay spread of the overall channel impulse response (CIR). It will be shown that this technique can provide superior performance compared to recent developments of equalizers, which are designed to maximize the impulse energy in a certain window. The performance of the proposed method is demonstrated for transmission on local loop twisted pairs. The design algorithm requires low computational complexity and is independent of the guard interval length. Simulation and analytical results visualize the performance of the new equalizer and compare it to those of a conventional equalizer.**

I. Introduction

Multicarrier modulation schemes such as Orthogonal Frequency Division Multiplex (OFDM) or Discrete Multi Tone (DMT) are currently applied in many applications e.g. digital audio broadcasting (DAB), digital terrestrial broadcasting (DVB-T) and asymmetrical digital subscriber line (ADSL). In such systems, a cyclically extended guard interval is inserted between successive multicarrier symbols to avoid intersymbol and interchannel interference (ISI, ICI). A channel impulse response (CIR) exceeding the duration of the given guard interval will cause ISI and ICI. To mitigate such effects, the idea is to feed the original CIR into a time domain equalizer (TEQ) such that the cascade of the composite channel and the equalizer yields an impulse response shorter than the guard interval. Recently, equalizers have been developed, which maximize the energy of the overall CIR in a given window [1]-[2]. In the subsequent we call such a solution an "energy equalizer". We propose and design a new equalizer, which directly minimizes the delay spread of the overall CIR ("delay spread equalizer").

II. System Model And Design Procedure

In this paper, a discrete representation of a OFDM/DMT system is assumed. The following parameters are considered:

- The length of the guard interval, represented by a cyclic prefix is G samples.
- The size of the discrete Fourier Transform (DFT) is N samples with $N \gg G$. Consequently, there is a maximum number of $N/2$ complex modulated carriers in a DMT system and N carriers in an OFDM system.
- The time base of the samples at the output of the transmitter is $T_A = 1/f_A = 1/2{,}208\ MHz$.
- Impulse response $h(n)$ of time invariant channel is of FIR type with length $K = 1024$ samples.
- The TEQ is an FIR-filter with impulse response $a(n)$ of length L_F samples.

The purpose of the TEQ is to minimize the delay spread of the overall CIR $h_{eff}(n)$ in an OFDM/DMT system, which is given by the convolution $h_{eff}(n) = h(n) * a(n)$. The parts of the overall CIR exceeding the guard interval cause ISI and ICI, depending on its distance to the guard interval and its energy [3]. In contrast to equalization techniques based on energy considerations as design criteria ("energy equalizer") [1]-[2], the "delay spread equalizer" incorporates the distance aspect.

The delay spread D of a discrete time function $h_{eff}(n)$ is defined as

$$D = \sqrt{\frac{1}{E} \cdot \sum_{n=-\infty}^{\infty} (n-\bar{n})^2 \cdot |h_{eff}(n)|^2} \geq 0 \qquad (1)$$

The energy E and the time center $\bar{n}$ of $h_{eff}(n)$ are given by

$$E = \sum_{n=-\infty}^{\infty} |h_{eff}(n)|^2 = \frac{1}{f_A} \cdot \int_{-\frac{f_A}{2}}^{\frac{f_A}{2}} \left| H_{eff}(e^{j2\pi f/f_A}) \right|^2 \cdot df \qquad (2)$$

$$\bar{n} = \frac{1}{E} \cdot \sum_{n=-\infty}^{\infty} n \cdot |h_{eff}(n)|^2 \qquad (3)$$

The overall CIR $h_{eff}(n)$ is given by the convolution of $h(n)$ with $a(n)$ and can be written in matrix notation as

$$\underbrace{\begin{bmatrix} h_{eff}(0) \\ h_{eff}(1) \\ \dots \\ h_{eff}(K+L_F-2) \end{bmatrix}}_{\vec{h}_{eff}} = \underbrace{\begin{bmatrix} h(0) & 0 & \dots & 0 \\ h(1) & h(0) & \dots & \dots \\ \dots & h(1) & \dots & 0 \\ h(K-1) & \dots & \dots & h(0) \\ 0 & h(K-1) & \dots & h(1) \\ \dots & \dots & \dots & \dots \\ 0 & 0 & \dots & h(K-1) \end{bmatrix}}_{\boldsymbol{H}} \cdot \underbrace{\begin{bmatrix} a(0) \\ a(1) \\ \dots \\ a(L_F-1) \end{bmatrix}}_{\vec{a}} \qquad (4)$$

Inserting (2) and (4) into (1) yields

$$D^2 = \frac{\vec{a}^H \cdot \boldsymbol{H}^H \cdot \boldsymbol{Q} \cdot \boldsymbol{H} \cdot \vec{a}}{\vec{a}^H \cdot \boldsymbol{H}^H \cdot \boldsymbol{H} \cdot \vec{a}} \qquad (5)$$

where $\boldsymbol{Q}$ is a diagonal matrix, containing the squared distances of the samples of $h_{eff}(n)$ from the time center $\bar{n}$.

IEEE International Conference on Communications, Conference Record pp. 1481-1485, Helsinki (Finland), June 2001

$$\boldsymbol{Q} = \begin{bmatrix} (0-\bar{n})^2 & & 0 \\ & \cdots & \\ & & \cdots \\ 0 & & ((K+L_F-2)-\bar{n})^2 \end{bmatrix} \tag{6}$$

D^2 is taken as cost function and has to be minimized. A good choice for the time center $\bar{n}$ of the effective CIR is $\bar{n} = \bar{n}_{orig}$, where $\bar{n}_{orig}$ denotes the time center of the original CIR $h(n)$. The expression in (5) leads to a quadratic optimization problem, where the denominator contains the energy of $h_{eff}(n)$. Therefore, the matrix product $\boldsymbol{H}^H \cdot \boldsymbol{H}$ results in a hermitian positive definite matrix and a Cholesky decomposition can be performed.

$$Chol\{\boldsymbol{H}^H \cdot \boldsymbol{H}\} = \boldsymbol{L}^H \cdot \boldsymbol{L} \tag{7}$$

The matrix $\boldsymbol{L}$ in (7) is an upper triangular matrix.
Furthermore, the substitutions

$$\vec{v} = \boldsymbol{L} \cdot \vec{a} \qquad \text{and} \qquad \vec{a} = \boldsymbol{L}^{-1} \cdot \vec{v} \tag{8}$$

are introduced. The insertion of (7) and (8) into (5) results in

$$D^2 = \frac{\vec{v}^H \cdot \boldsymbol{W} \cdot \vec{v}}{\vec{v}^H \cdot \vec{v}} \tag{9}$$

with

$$\boldsymbol{W} = (\boldsymbol{L}^{-1})^H \cdot \boldsymbol{H}^H \cdot \boldsymbol{Q} \cdot \boldsymbol{H} \cdot \boldsymbol{L}^{-1} \tag{10}$$

In mathematics, the term on the right hand side of (9) is known as Rayleigh-quotient. It is independent of the absolute value of $\vec{v}$ and ranges between the smallest and the largest eigenvalue, μ_{min} and μ_{max}, of the hermitian matrix $\boldsymbol{W}$ [4]. Consequently, the minimum delay spread is given by

$$D_{min} = \sqrt{\mu_{min}}. \tag{11}$$

To obtain D_{min}, $\vec{v}$ has to be chosen as the eigenvector corresponding to μ_{min}. The coefficient vector $\vec{a}$ of the "delay spread equalizer" can then be calculated by using (8).

III. Simulation And Computation Results

We have analyzed the performance of the described delay spread equalization method in a DMT transmission system over a twisted pair subscriber loop. Hence, the CIR $h(n)$ is assumed to be real-valued. As a consequence, real-valued equalizer coefficients are sufficient. The results of the proposed equalizer are compared with those of the "energy equalizer" [1], [2].
In Fig. 1, the CIR of a subscriber loop with 3 km length and 0,4 mm wire diameter as well as the corresponding compressed impulse responses for both types of equalization are shown. A cyclic prefix with $G = 16$ samples is assumed. The effective CIR, obtained by the "delay spread equalizer" is denoted by $h_{eff_1}(n)$. In contrast to that, $h_{eff_2}(n)$ denotes the effective CIR obtained by the "energy equalizer". The compressing effect of the TEQ is clearly visible for both equalization techniques. The maximum length $G+1$ of the CIR to avoid ISI/ICI in the DMT system is marked with grey color in the subplots of Fig. 1. The delay spread of the overall CIR $h_{eff}(n)$ is about $4\mu s$ without time domain equalization. It is reduced to $1\mu s$ with the "energy equalizer" and even to $0{,}5\,\mu s$ with the proposed "delay spread equalizer".

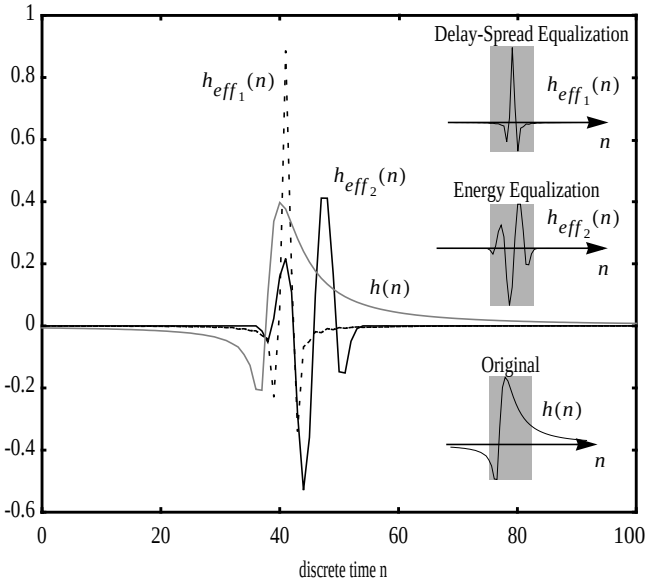

Fig. 1: Normalized CIR $h(n)$ of a subscriber loop (length 3 km, wire diameter 0,4 mm) without equalization. $h_{eff_1}(n)$ is the CIR with minimized delay spread and $h_{eff_2}(n)$ is the compared CIR compressed with method [2].

A. Interference Power

In the following, we give an approximation similar to [3] to estimate the ISI/ICI power of the subchannels at the output of the DFT filter bank at the receiver. For this purpose, we chose a window of size $G+1$, that covers as much energy of the overall CIR $h_{eff}(n)$ as possible. The samples outside of the window are denoted pre- and postcursors. They contribute to the ISI and ICI power. According to Fig. 2, we define the impulse responses $w_{pre,\vartheta}(n)$ $(\vartheta = 1, \ldots, P_1)$ and $w_{post,\xi}(n)$ $(\xi = 1, \ldots, P_2)$ of the pre- and postcursor, which remain outside the window of $G+1$ consecutive samples. The numbers P_1 and P_2 of such impulse responses are determined by the length of the cyclic prefix and the overall CIR $h_{eff}(n)$. Furthermore, the maximum length of $w_{pre,\vartheta}(n)$ and $w_{post,\xi}(n)$ is given by the size N of the DFT. The transmitter signal of the DMT system can be assumed as zero mean and white Gaussian process, if nearly all carriers are modulated with uncorrelated symbols of equal power σ_{xx}^2. Then, an approximation for the ISI/ICI power $\sigma_{inter,m}^2$ of the m^{th} subchannel $(m = 0, 1, \ldots N-1)$ is given by (12).

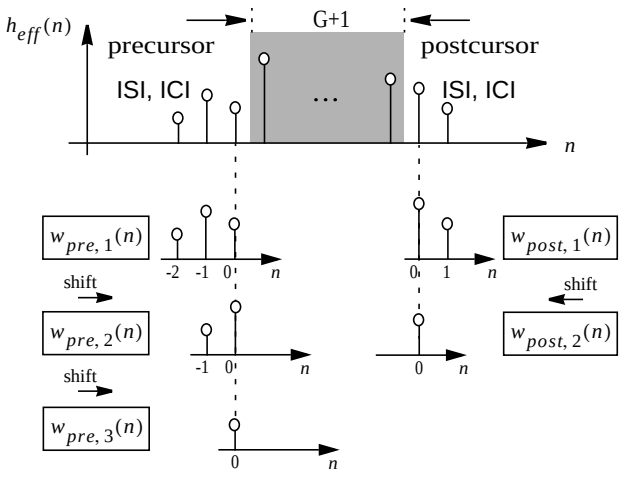

Fig. 2: ISI and ICI due to pre- and postcursor of the CIR $h_{eff}(n)$ at the DMT-receiver.

$$\sigma^2_{inter,m} = \sigma^2_{xx} \cdot \sum_{\nu=-(N-1)}^{N-1} \left(1 - \frac{|\nu|}{N}\right) \cdot z(\nu) \cdot e^{-j\frac{2\pi}{N}m\nu} \tag{12}$$

$$z(\nu) = \frac{2}{N} \cdot \left\{ \sum_{\vartheta=1}^{P_1} w_{pre,\vartheta}(\nu) * w_{pre,\vartheta}(-\nu) \right\} + \frac{2}{N} \cdot \left\{ \sum_{\xi=1}^{P_2} w_{post,\xi}(\nu) * w_{post,\xi}(-\nu) \right\} \tag{13}$$

The convolution in (13) is denoted by „*“. Fig. 3 shows the ISI/ICI power of the m^{th} subchannel of a DMT system for both equalization methods. Transmission over a twisted pair subscriber loop with 3 km length and 0,4 mm wire diameter is considered. As a result, the ISI/ICI power of all subchannels decreases by more than 30 dB for both equalization techniques. A comparison with the simulated results in Fig. 3 shows, that (12) provides quite acceptable results.

B. Impact of Channel Noise

Time domain equalization changes noise properties at the receiver. Parts of the DMT receiver are shown in Fig. 4. We examined the noise power $\sigma^2_{noise,m}$ at the m^{th} subchannel output of the DFT filter bank in presence of zero mean additive white Gaussian noise (AWGN) with variance σ^2_{AWGN} on the channel as shown in Fig. 4. Neglecting the removal of the guard interval, $\sigma^2_{noise,m}$ can be calculated by (14) and (15) [5].

$$\sigma^2_{noise,m} = \sigma^2_{AWGN} \cdot \sum_{\nu=-(N-1)}^{N-1} \left(1 - \frac{|\nu|}{N}\right) \cdot c(\nu) \cdot e^{-j\frac{2\pi}{N}m\nu} \tag{14}$$

$$c(\nu) = a(\nu) * a(-\nu) = \sum_{k=-\infty}^{\infty} a(k) \cdot a(k-\nu) \tag{15}$$

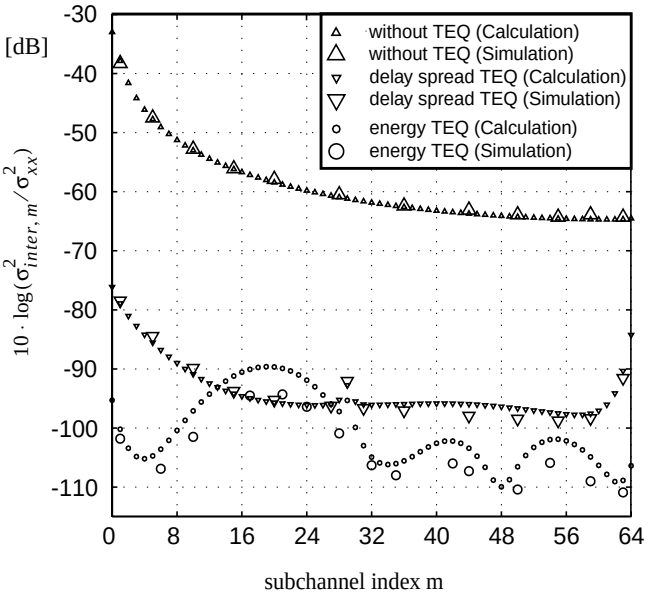

Fig. 3: ISI/ICI power of m^{th} subchannel of a DMT receiver with $G = 16$ and $N = 128$. Subscriber loop with 3 km length, 0,4 mm wire diameter, TEQ with $L_F = 16$ coefficients.

According to (14) and (15), $\sigma^2_{noise,m}$ depends on the equalizer coefficients $a(n)$. Simulation and analytical results for the noise power $\sigma^2_{noise,m}$ are shown in Fig. 5. As can be seen, simulation results confirm (14) quite well. Further, Fig. 5 illustrates, that the white channel noise becomes colored after time domain equalization. As a consequence, the variance $\sigma^2_{noise,m}$ of the noise changes from subchannel to subchannel.

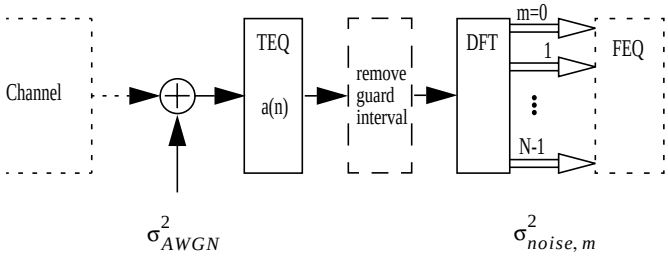

Fig. 4: DMT receiver with TEQ and noisy channel.

C. Signal-to-distortion ratio

As long as the guard interval is of adequate length, the signal power at the m^{th} output channel of the DFT is given by (16). It is assumed, that the transmitter modulates all carriers with equal power σ^2_{xx}.

$$\sigma^2_{signal,m} = \sigma^2_{xx} \cdot |\lambda_m|^2 \tag{16}$$

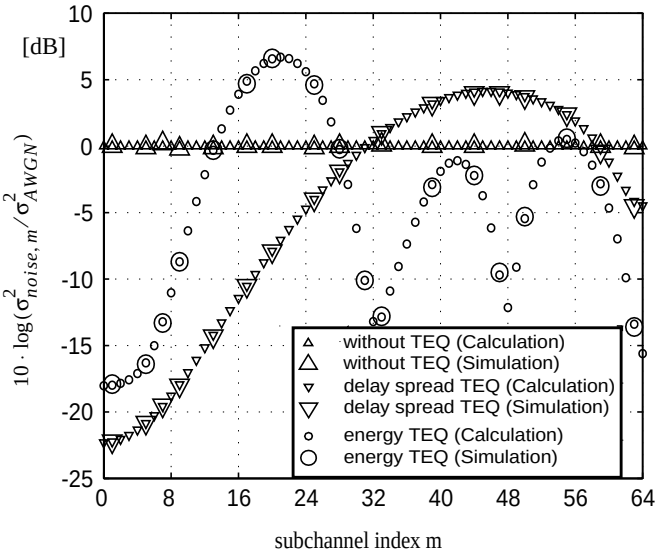

Fig. 5: Output noise power of m^{th} subchannel of a DMT receiver with $G = 16$ and $N = 128$ in presence of AWGN at the input of the receiver. TEQ with $L_F = 16$ coefficients.

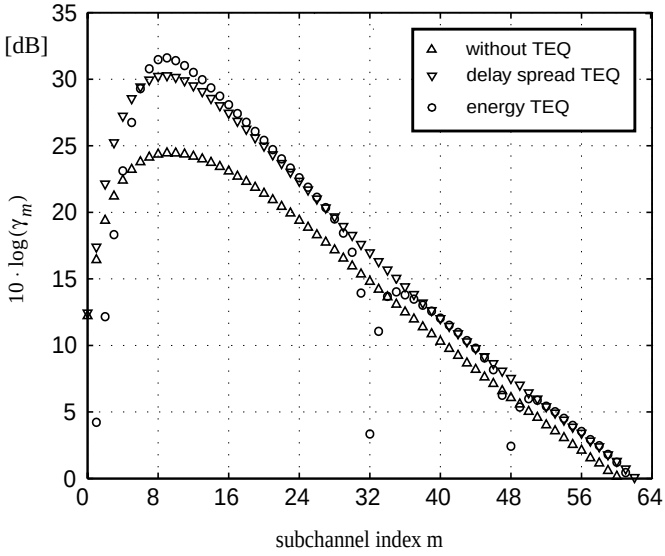

Fig. 6: Signal-to-distortion ratio γ_m at the output of the m^{th} subchannel of a DMT receiver with $N = 128$, $G = 16$ and $\sigma^2_{AWGN}/\sigma^2_{xx} = 10^{-6}$. Subscriber loop with 3 km length, 0,4 mm wire diameter, TEQ with $L_F = 16$ coefficients.

The parameter $|\lambda_m|$ in (16) denotes the magnitude of the overall transfer function of the m^{th} subchannel, specified by the channel and the equalizer transfer function.

The ISI/ICI power is assumed to be small compared to the signal power at the receiver. Considering the ISI/ICI power (12), the noise power (14) and the signal power (16), the signal-to-distortion ratio γ at the output of the m^{th} subchannel of the DMT receiver is given by

$$\gamma_m = \frac{|\lambda_m|^2}{\sum_{\nu=-(N-1)}^{N-1} \left(1 - \frac{|\nu|}{N}\right) \cdot \left[z(\nu) + \frac{\sigma^2_{AWGN}}{\sigma^2_{xx}} c(\nu) \right] \cdot e^{-j\frac{2\pi}{N} m\nu}} \qquad (17)$$

The signal-to-distortion ratio γ_m with and without time domain equalization is shown in Fig. 6 for transmission over a twisted pair subscriber loop of 3 km length. Apart from the notches, present with the "energy equalizer", γ_m is increased in most subchannels for both equalization methods due to the reduction of ISI/ICI. However, notches are present in the γ_m function when the energy equalization method is applied. In contrast to that, there occur no notches by the "delay spread equalizer". The effect of such notches is a performance degradation of the transmission system.

As a measure for improvement, we use the geometric mean of γ_m, averaged over all subchannels. This value improves from 13,6 dB without TEQ to 15,0 dB with energy equalization and even to 16,2 dB with delay spread equalization. The impact of γ_m on the achievable data rate is for further study.

D. Impact of synchronization error

A critical problem of OFDM/DMT systems is given by symbol timing at the receiver [6]. For this purpose, the sensitivity against synchronization errors at the receiver is examined for both equalization methods. Fig. 7 visualizes the ISI/ICI power of the m^{th} subchannel as a function of synchronization offset by transmission over a subscriber loop of 3 km length, when equalization is done with the conventional „energy equalizer“.

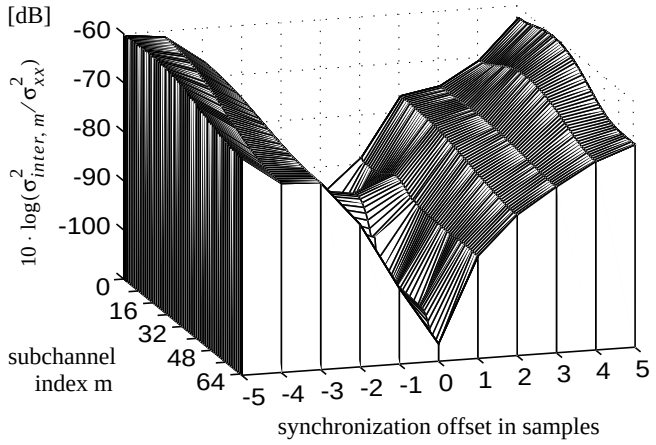

Fig. 7: ISI/ICI power at the receiver due to synchronization offset by using the energy equalization method. DMT modulation with $N = 128$ and $G = 16$. Subscriber loop with 3 km length, 0,4 mm wire diameter, TEQ with $L_F = 16$ coefficients.

It can be seen, that ISI/ICI power rises enormously, when symbol timing is not ideal. So we can recognize, that the system with the "energy equalizer" is rather sensitive against synchronization error. In contrast to that, the system with the delay spread equalization method is relatively insensitive, as it is shown in Fig. 8. For various synchronization errors, a direct comparison of the ISI/ICI power between both equalization methods is illustrated in Fig. 9 as a contour plot.

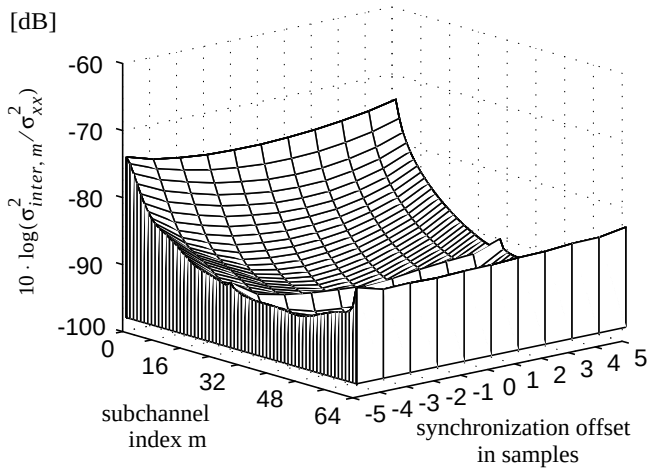

Fig. 8: ISI/ICI power at the receiver due to synchronization offset by using the delay spread equalization method. DMT modulation with $N = 128$ and $G = 16$. Subscriber loop with 3 km length, 0,4mm wire diameter, TEQ with $L_F = 16$ coefficients.

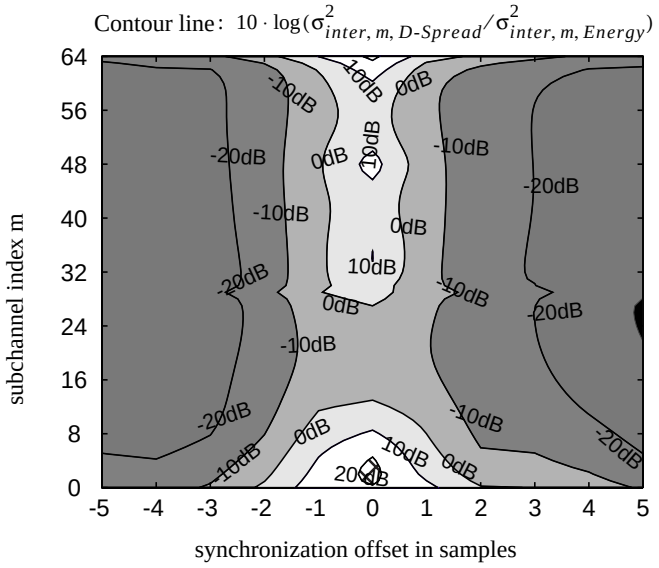

Fig. 9: Comparison of ISI/ICI power between "delay spread equalizer" and "energy equalizer" in the subchannels of a DMT receiver with $N = 128$ and $G = 16$ as a function of synchronization offset. Subscriber loop with 3 km length, 0,4 mm wire diameter, TEQ with $L_F = 16$ coefficients.

Assuming ideal symbol timing, ISI/ICI power is lower in most subchannels by using the "energy equalizer". However, in presence of synchronization errors, the ISI/ICI power with the "delay spread equalizer" rises much less with increasing synchronization offset than with the "energy equalizer". Consequently, the penalty in system performance due to synchronization error is much lower by using the delay spread equalization method.

IV. Conclusion

We have designed an equalizer which minimizes the delay spread in an OFDM/DMT system. The solution was applied on a twisted pair subscriber line with 3 km length and 0,4 mm wire diameter. As a result, the equalizer can reduce the ISI/ICI power in the DMT subchannels significantly. The solution was compared to an "energy equalizer" which maximizes the energy of the overall CIR in a certain window. It was demonstrated, that time domain equalization changes noise properties at the receiver. Considering noise and ISI/ICI together as distortion, the proposed "delay spread equalizer" can achieve a higher signal-to-distortion ratio than the "energy equalizer". Furthermore, we have examined the performance of the new equalizer in the presence of symbol synchronization offsets at the receiver. It was demonstrated, that the performance degradation due to synchronization errors is lower with the delay spread equalization method than with the energy equalization method. Already for a timing offset of about 2 samples, the difference in ISI/ICI power between both equalization methods is more than 10 dB in most subchannels.

References

[1] J. W. Melsa, R. C. Younce, C. E. Rohrs, "Impulse Response Shortening for discrete Mutlitone Transceivers," *IEEE Trans. on Comm.*, No. 12, Dec. 1996

[2] R. Schur, J. Speidel, R. Angerbauer, "Reduction of Guard Interval by Impulse Compression for DMT Modulation on Twisted Pair Cables," *Proceedings of IEEE GLOBECOM '00*, San Francisco, Vol. 3, pp. 1632-1636, Nov. 2000

[3] J. L. Seoane, S. K. Wilson, S. Gelfand, "Analysis of Intertone and Interblock Interferences in OFDM when the length of the cyclic Prefix is shorter than the length of the Impulse Response of the channel," *Proceedings of IEEE GLOBECOM '97*, Phoenix, Vol. 1, pp. 32-36, Nov. 1997

[4] H. R. Schwarz, H. Rutishauser, E. Stiefel, "*Numerik symmetrischer Matrizen*" (in german), Teubner-Verl., 1968

[5] S. Kapoor, S. Nedic, "Interference Suppression in DMT Receivers using Windowing," *Proceedings of IEEE ICC '00*, New Orleans, Vol. 2, pp. 778-782, June 2000

[6] T. Pollet, M. Peeters, "Synchronization with DMT Modulation," *IEEE Communications Magazine*, pp. 80-86, No. 4, Apr. 1999